

K, whence $2\theta/\delta \approx 4$, taking $\theta = 3.6$ K from Ref. 6.

³G. H. Lander, T. O. Brun, J. P. Desclaux, and A. J. Freeman, Phys. Rev. B 8, 3237 (1973).

¹⁰See, e.g., M. Born and K. Huang, *Dynamical Theory of Crystal Lattices* (Oxford Univ. Press, Oxford, England, 1954), Sec. 30.

Effect of Stress on High-Field Magnetoresistance Anisotropy Due to Open Orbits in Iron*

M. A. Angadi,[†] E. Fawcett, and Mark Rasolt

Department of Physics, University of Toronto, Toronto, Ontario, Canada

(Received 26 December 1973)

The effect of uniaxial stress on the high-field magnetoresistance anisotropy of iron is measured and shown, by a combination of group theory and a band-structure interpolation scheme, to correspond to the origin of the $\langle 100 \rangle$ open orbits being magnetic breakdown between the hole octahedron and the electron jack on the minority-spin Fermi surface.

The magnetoresistance anisotropy curves for iron show deep minima due to open orbits in $\langle 100 \rangle$ and $\langle 110 \rangle$ directions.^{1,2} Wakoh and Yamashita³ proposed that the $\langle 110 \rangle$ open orbits occur along the $\langle 110 \rangle$ arms of a multiply connected hole sheet of the majority-spin Fermi surface which appears in their energy-band structure. Gold *et al.*⁴ showed that a rigid exchange splitting of the energy bands of Wood⁵ for paramagnetic iron results in the hole arms being pinched off as a result of hybridization with the electron surface centered on Γ . However, because of the magnetic breakdown the resultant surfaces (I and II in Fig. 1) are likely still to support open orbits along $\langle 110 \rangle$. Falicov and Ruvalds⁶ showed that an accidental degeneracy, such as that at points i_1 and i_2 , is allowed only when \vec{B} is along a symmetry axis and the points are in a symmetry plane perpendicular to \vec{B} as in Fig. 1. When \vec{B} is tilted away from z in the (110) plane, the probability of breakdown at i_1 and therefore the number of open orbits should decrease as the degeneracy is progressively lifted by spin-orbit interaction. This is consistent with the observed angular dependence of the depth of the magnetoresistance minima associated with $\langle 110 \rangle$ open orbits.

In this Letter we are primarily concerned with the origin of the $\langle 100 \rangle$ open orbits. Wakoh and Yamashita³ suggested that they result from breakdown between the minority-hole octahedron and electron jack. They further pointed out that their multiply connected majority-hole surface would support $\langle 100 \rangle$ (as well as $\langle 110 \rangle$) open orbits for \vec{B} within 8° from a $\langle 100 \rangle$ axis, but these

are unlikely to exist to any appreciable extent for the Fermi surface in Fig. 1.

Since uniaxial stress breaks the cubic symmetry, it will remove degeneracies in certain symmetry planes and directions, while leaving accidental degeneracies unresolved. We have therefore employed stress to determine whether

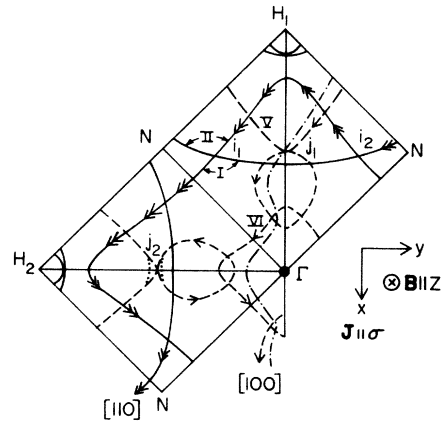


FIG. 1. Fermi surface of iron in (001) plane (after Gold *et al.*, Ref. 4) showing the splitting of levels at j_2 on the ΓH_2 line parallel to y resulting from uniaxial stress along x ; solid line, majority surface; dashed line, minority surface; dash-dotted line, open orbit along $\langle 100 \rangle$ when \vec{B} is rotated a few degrees away from z in the (100) plane; dashed arrows, open orbits along $[100]$ resulting from the stress-induced splitting at j_2 ; solid arrows, open orbits along $[110]$ resulting from breakdown between the majority large electron surface I and the hole arms II at i_1 and i_2 . Spin-orbit splitting is not shown, though it is necessary to include spin-orbit interaction for breakdown to occur at j under zero stress, as explained in the text.

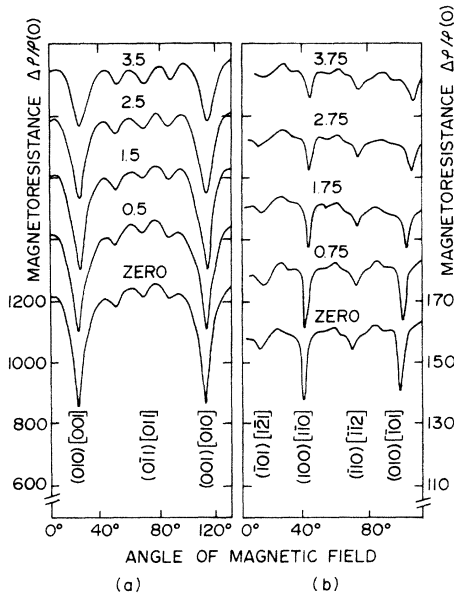


FIG. 2. Transverse magnetoresistance rotation curves for iron whiskers under various tensions (for clarity each curve for successively increasing tension is shifted by one division). (a) $\sigma \parallel \mathbf{J} \parallel [100]$, whisker dimensions $0.26 \times 0.24 \times 8 \text{ mm}^3$, residual resistivity ratio = 1920, $T = 4.2 \text{ K}$, $B = 120 \text{ kG}$; 3.5 kg tension gives $\approx 0.26\%$ longitudinal strain. (b) $\sigma \parallel \mathbf{J} \parallel [111]$, whisker diameter 0.34 mm, residual resistivity ratio > 860 , $T = 4.2 \text{ K}$, $B = 120 \text{ kG}$; 3.75 kg tension gives $\approx 0.25\%$ longitudinal strain. The identification of the minima as [100] (010) etc. indicates the directions of \vec{B} and the open orbit, respectively.

the origin of the open orbits in iron is consistent with the above picture. The sample holder used to apply stress while rotating the sample in the field of a superconducting solenoid was described in an earlier publication,⁷ where preliminary results for iron were reported. The experimental data in Fig. 2 show that in both [100] and [111] samples the $\langle 100 \rangle$ minima are sensitive to stress, whereas the $\langle 110 \rangle$ minima are not affected by stress to within experimental accuracy. The change in depth of the $\langle 100 \rangle$ minima is linear as a function of stress and reversible (and therefore not due to plastic deformation of the whisker).

We first note that it is necessary to include the spin-orbit interaction to obtain magnetic breakdown at j in Fig. 1, since the wave functions on the minority-hole octahedron and electron jack at this point are orthogonal.⁸ However, apart from assuming magnetic breakdown at j , we neglect the spin-orbit interaction in our calculation since, as we shall see, the effect of uniaxial stress is to change the connectivity of the minor-

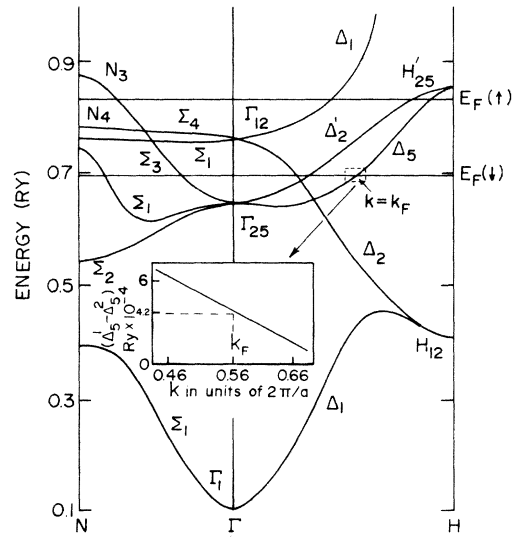


FIG. 3. Energy bands of Wood (Ref. 5) with the branches Δ_2 and Δ_2' depressed slightly to give the neck and lens sheet of the minority surface. The inset shows the splitting $\Delta_5^1 - \Delta_5^2$ plotted against the wave vector \vec{k} near the Fermi level \vec{k}_F resulting from the maximum uniaxial stress $\sigma \parallel [100]$ and corresponding to Eq. (6).

ity surface in such a way as to decrease the number of $\langle 100 \rangle$ open orbits independently of the nature of the spin-orbit splitting. We note that the insensitivity to uniaxial stress of the $\langle 110 \rangle$ minima in Fig. 2 is consistent with their origin through breakdown at points of accidental degeneracy (i in Fig. 1), since changes of crystal symmetry due to stress will not remove such degeneracies. On the other hand the $\langle 100 \rangle$ open orbit shown in Fig. 1 results from breakdown at points j on a symmetry axis, where degeneracy results from symmetry and is therefore likely to be sensitive to stress. We consider first the observed behavior shown in Fig. 2(a), that the depth of the minimum in the magnetoresistance for \vec{B} along a cube axis decreases with stress σ and current \vec{J} both along the perpendicular cube axis (i.e., the configuration shown in Fig. 1). Two possible effects of stress are consistent with this result: (a) Points j_1 and j_2 both split in such a way as to create closed electron and hole orbits, resulting in compensation and therefore a high magnetoresistance. (b) Point j_2 splits in such a way (dotted line in Fig. 1) as to create an open orbit (dashed-arrow lines in Fig. 1) along $\vec{J} \parallel x$, resulting again in a high magnetoresistance. In relation to case (b), we note that if contact at j_2 were to be removed in such a way (the opposite to that shown in Fig. 1) that the

hole surface penetrated the electron surface, then breakdown at j_2 would increase and the magnetoresistance minimum would become deeper (or at least remain unchanged).

Possibility (a) can be discounted, since for strain along x axis j_1 remains doubly degenerate. We now demonstrate that possibility (b) does occur since (i) the contact at j_2 is removed or (ii) the contact is removed in such a way as to produce the dotted curve in Fig. 1. Condition (i) is satisfied because the point group for j_2 changes to the operations

$$E \equiv x \rightarrow x, y \rightarrow y, z \rightarrow z;$$

$$C_2 \equiv x \rightarrow -x, y \rightarrow y, z \rightarrow -z;$$

$$JC_2^a \equiv x \rightarrow x, y \rightarrow y, z \rightarrow -z;$$

$$JC_2^b \equiv x \rightarrow -x, y \rightarrow y, z \rightarrow z;$$

giving the character table

	E	C_2	JC_2^a	JC_2^b
Δ_1	1	1	1	1
Δ_2'	1	1	-1	-1
Δ_5^1	1	-1	-1	1
Δ_5^2	1	-1	1	-1

so that $\Delta_5 - \Delta_5^1, \Delta_5^2$. Now condition (ii) is equivalent to the inequality $\Delta_5^1 > \Delta_5^2$ for the point j_2 in Fig. 1, as may be seen by noting group-theoretical compatibility relations, $\Delta_5^1 \rightarrow \Sigma_3$ and $\Delta_5^2 \rightarrow \Sigma_1$, as we move from k along ΓH to k along ΓN in Fig. 3. This inequality may be shown to follow from Wood's⁵ calculation by use of a band-structure interpolation scheme.

Now (1) noting that j_2 lies approximately at the center of ΓH so that the main contribution from $|\psi_{\vec{k}+\vec{c}}\rangle$ ⁹ comes from $\vec{G}=0$, (2) making use of (1) and the characters of Δ_5^1 and Δ_5^2 , and (3) using Slater and Koster⁹ overlap integrals corresponding to the position under uniaxial stress of the first and second nearest neighbors, we obtain to first order in δa

$$\Delta_5^1(0, \mathbf{k}, 0) - \Delta_5^2(0, \mathbf{k}, 0) = \frac{16}{9} \cos(ka/2) \gamma (1 + \beta) [-3dd\sigma_1(s) + dd\pi_1(s) + 2dd\delta_1(s)] + 2(1 + \beta) \gamma a [dd\delta_2'(a) - dd\pi_2'(a)], \quad (1)$$

where $s = (\sqrt{3}/2)a$, longitudinal strain $\gamma \equiv \delta a/a$, Poisson ratio $\beta \equiv \delta b/\delta a$, the subscripts denote first and second nearest neighbor, and the prime means differentiation with respect to a . Second-nearest-neighbor contributions are included in Eq. (1) since they correspond to actual displacements of the atoms, whereas nearest-neighbor contributions correspond only to change in orientation, and also because for $k \approx k_F$ along ΓH in Fig. 3, $ka/2 \approx \pi/2$, so that $\cos(ka/2)$ is small. Similar considerations show that next-nearest-neighbor and higher contributions can be neglected.

The disposable parameters of Eq. (1) are evaluated by noting first that for our purposes $\Delta_5, \Delta_2', \Sigma_2, \Sigma_3$, and Σ_4 are all pure d -like representations so that applying the above procedure to the bcc lattice we get

$$\Delta_5(0, \mathbf{k}, 0) = d_0 + \frac{8}{3} \cos(ka/2) [dd\sigma_1(s) + \frac{2}{3} dd\pi_1(s) + \frac{4}{3} dd\delta_1(s)], \quad (2)$$

$$\Sigma_3(\mathbf{k}, \mathbf{k}, 0) = d_0 + \frac{4}{3} [1 + \cos(ka)] [dd\sigma_1(s) + \frac{2}{3} dd\pi_1(s) + \frac{4}{3} dd\delta_1(s)] + \frac{4}{3} [1 - \cos(ka)] [-dd\sigma_1(s) + \frac{1}{3} dd\pi_1(s) + \frac{2}{3} dd\delta_1(s)], \quad (3)$$

$$\Sigma_4(\mathbf{k}, \mathbf{k}, 0) = d_0 + \frac{4}{3} [1 + \cos(ka)] [2dd\pi_1(s) + dd\delta_1(s)]. \quad (4)$$

To get $dd\delta_2(a)$ and $dd\pi_2(a)$ we exploit the fact that Δ_2' and Δ_5 are degenerate to first nearest neighbors, so that

$$\Delta_2'(0, \mathbf{k}, 0) - \Delta_5(0, \mathbf{k}, 0) = 2[1 - \cos(ka)] [dd\pi_2(a) - dd\delta_2(a)]. \quad (5)$$

We note from Fig. 3 and Eq. (5) that $dd\pi_2(a) - dd\delta_2(a) > 0$, also that $|dd\delta_2(a)|$ and $|dd\pi_2(a)|$, being overlap integrals,⁹ are monotonically decreasing functions of a in the range of interest. Hence $dd\delta_2'(a) - dd\pi_2'(a) > 0$, so that the last term of Eq. (1) is positive.

Finally, we estimate its size by noting that the functional form is dominated by $e^{-a/\lambda}$, where λ is a bit larger than the exponential tail of the $3d$ atomic wave function for iron (i.e., $\lambda \approx 0.88a_0$, $a_0 \equiv$ Bohr radius). For marginal safety we use $\lambda = a_0$, and substituting in Eq. (5) the Poisson ratio $\beta = 0.28$ for

Fe and the strain $\gamma = 2.5 \times 10^{-3}$ corresponding to the maximum [100] stress in Fig. 2(a), we get

$$\Delta_5^1(0, k, 0) - \Delta_5^2(0, k, 0) = [8.1 \cos(ka/2) + 5.6] 10^{-4} \text{ Ry.} \quad (6)$$

This result is plotted in the inset of Fig. 3, and we see that at $k = k_F$ we have $\Delta_5^1 > \Delta_5^2$. This implies condition (ii), i.e., uniaxial stress $\sigma_{\parallel}[100]$ removes the contact at j_2 between the electron and hole surfaces in such a way as to produce the dotted curve in Fig. 1.

From Eq. (6) we find that the maximum [100] stress, which produces about 50% reduction in the depth of the $\langle 100 \rangle$ minima in Fig. 2(a), corresponds for the value $k_F = 0.56(2\pi/a)$ (Fig. 3) to an energy splitting $\Delta_5^1 - \Delta_5^2 = 4.2 \times 10^{-4}$ Ry. This would be too small to produce a significant change in the breakdown along a line in a symmetry plane, the case considered in the previous theoretical treatments of magnetic breakdown.¹⁰ But the present case is very different: Contrary to the assumption of previous authors,²⁻⁴ there is no breakdown at the degeneracy point on a symmetry axis, such as the point contact j between the electron and hole surfaces in Fig. 1, in the absence of spin-orbit interaction.⁸ We conclude that the nature of the spin-orbit splitting at j must be such as to result in breakdown at zero stress, which will disappear when the stress-induced energy splitting, given by Eq. (1), sufficiently separates the electron and hole surfaces.

Finally, we remark that the minima associated with $\langle 100 \rangle$ open orbits in Fig. 2(b) for $\sigma_{\parallel}[111]$ are even more sensitive to stress than in Fig. 2(a) for $\sigma_{\parallel}[100]$. Although we have not done the calculations for $\sigma_{\parallel}[111]$, we can predict from group theory that both contacts j_1 and j_2 in Fig. 1 will be removed, resulting in closed electron and hole orbits, which restores compensa-

tion and therefore gives a high magnetoresistance.

In conclusion our experiments confirm the picture of the Fermi surface which is emerging from recent de Haas-van Alphen measurements^{4,11} and our calculation can be seen not to depend upon accidental features of the energy-band structure of iron.

We wish to acknowledge stimulating discussions with Professor L. M. Falicov.

*Work supported by the National Research Council of Canada.

†On study leave from Karnatak University, Dharwar-3, Karnatak State, India.

¹W. A. Reed and E. Fawcett, Phys. Rev. **136**, A422 (1964).

²R. V. Coleman, R. C. Morris, and D. J. Sellmyer, Phys. Rev. B **8**, 317 (1973).

³S. Wakoh and I. Yamashita, J. Phys. Soc. Jap. **21**, 1712 (1966).

⁴A. V. Gold, L. Hodges, P. T. Panousis, and D. R. Stone, Int. J. Magn. **2**, 357 (1971).

⁵J. H. Wood, Phys. Rev. **126**, 517 (1962).

⁶L. M. Falicov and J. Ruvalds, Phys. Rev. **172**, 498 (1968).

⁷M. A. Angadi, D. E. Britton, and E. Fawcett, J. Phys. E: J. Sci. Instrum. **6**, 1086 (1973).

⁸L. M. Falicov and E. I. Blount, private communications.

⁹J. C. Slater and G. F. Koster, Phys. Rev. **94**, 1498 (1954).

¹⁰E. I. Blount, Phys. Rev. **126**, 1636 (1972).

¹¹D. R. Baraff, Phys. Rev. B **8**, 3439 (1973).